Pergamon

Int. J. Solids Structures Vol. 32, No. 6/7, pp. 817–826, 1995

0020-7683/95 $9.50 + .00

0020-7683(94)00162-6

DETERMINATION OF MECHANICAL SPECTRA FROM EXPERIMENTAL RESPONSES

I. EMRI
University of Ljubljana, SLO-61000 Ljubljana, Slovenia

and

N. W. TSCHOEGL
California Institute of Technology, Pasadena, CA 91125, U.S.A.

(*Received* 30 *December* 1993; *in revised form* 26 *May* 1994)

Abstract—A recursive computer algorithm was developed which generates line spectra from experimental response functions. The method allows storing information on the mechanical properties of polymeric materials in a convenient way. The algorithm also interconverts between relaxation and retardation spectra. From the spectra, any desired response function can then be recovered. The algorithm essentially utilizes the fact that the kernel functions resemble step functions. Slightly different codes are used for each kernel function. The appearance of negative relaxation or retardation lines is obviated. Mathematically such lines would be acceptable, and they do not seriously affect reconstruction of responses within relaxation or retardation behavior. However, they would seriously interfere with interconversion between the two types of behavior, and they would also pose problems in the interpretation of the spectra.

INTRODUCTION

In the response of a linearly viscoelastic material to a strain excitation, complete information on the time-dependent part of the response is contained in the relaxation spectrum. In the response to a stress excitation, the same role is played by the retardation spectrum. The response then consists of the appropriate viscoelastic constants (such as the equilibrium modulus, or the glass compliance and the steady flow fluidity), in addition to the integral over the spectrum multiplied by a kernel function characteristic of the type of excitation chosen to elicit the response. If this is a strain or a stress as a step function of time, the result is the relaxation modulus in the first, and the creep compliance in the second case. Thus, once the spectrum is known in addition to the viscoelastic constants, it is possible to generate from it the response to any desired type of excitation.

The spectrum itself is not accessible by direct experiment. From a theoretical response curve it can often be calculated exactly (Tschoegl, 1989, Chapter 6). From experimental data the spectrum is necessarily obtained as an approximation to the true spectrum. A variety of methods have been proposed (Tschoegl, 1989, Chapter 4; Ferry, 1980) to extract approximations to the spectra from experimental data by mathematical manipulation. The well known methods based on numerical or graphical differentiation typify this approach. In another approach, an attempt is made to determine a distribution of discrete spectral lines from which the original response curve can be more or less faithfully reproduced (Tschoegl, 1989, Chapter 3, Section 6). Among the better known older methods are Procedure X of Tobolsky and Murakami (1959), the collocation method of Schapery (1962), and an extension of it by Cost and Becker (1970) which they call the multidata method. The last two named methods require matrix inversion. Both are likely to generate negative spectrum lines, which make it virtually impossible to use this spectrum for interconversion between the relaxation and retardation behavior. In the past few years several new papers have been devoted to this subject (Laun, 1986; Baumgaertel and Winter, 1989; Honercamp, 1989; Honercamp and Weese, 1989; Kamath and Mackley, 1989; Elster and Honercamp, 1991, 1992; Orbey and Dealy, 1991; Janzen and Scanlan, 1992). An extensive comparison

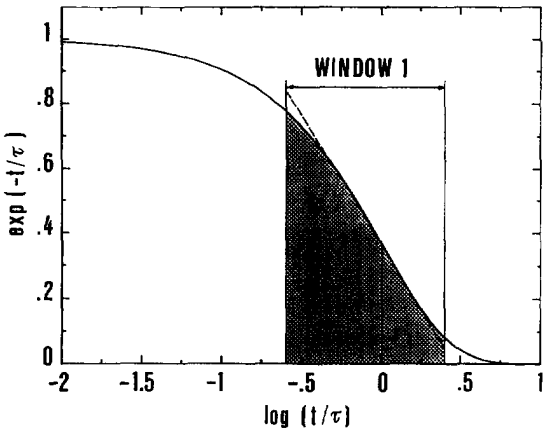

Fig. 1. Definition of window 1 (the boundary window).

of these methods along with the method introduced here is presented elsewhere (Emri and Tschoegl, 1995).

We present here the method based on an iterative computer algorithm for calculating a distribution of spectral lines which, for a given set of data, is unique within the desired degree of accuracy. It must be emphasized that the discrete distribution of moduli or compliances on respondence (relaxation or retardation) times obtained in this way is still an approximation. However, as will be shown below, the calculated distributions appear to yield better results than any of the other methods.

In this paper we shall sketch only the application of the algorithm to the relaxation modulus. The power of the algorithm will then be demonstrated on the experimental data obtained by Catsiff and Tobolsky (1955). These data were originally reported in terms of the tensile modulus $E(t)$. For the comparison reasons presented in Emri and Tschoegl (1993), the data were first converted to the shear modulus, as reported in Tschoegl (1989, p. 40). For the same reason the units of the modulus were converted from dynes/cm^2 and hours to N/m^2 and seconds.

A complete presentation of the algorithm has been published elsewhere, in a series of four papers (Emri and Tschoegl, 1993a; Emri and Tschoegl, 1993b; Tschoegl and Emri, 1992; Emri and Tschoegl, 1994). The first paper in this series, Emri and Tschoegl (1993a), describes the algorithm for obtaining a discrete distribution of relaxation times from simulated relaxation modulus data, or of retardation times from simulated creep compliance data. The second paper, Emri and Tschoegl (1993b), deals with the determination of the spectra from theoretical storage and loss functions. The third paper, Tschoegl and Emri (1992), takes up the problem of converting between relaxation modulus and creep compliance. In these first three papers, the algorithm has been thus applied to data sets obtained by sampling continuous theoretical curves. This has simplified presentation of the details and the power of the algorithm. The fourth paper, Emri and Tschoegl (1994), deals finally with the application of our method to experimental data, i.e. data that are not free of experimental error.

THEORETICAL

Essentially the method consists of predetermining a set of respondence times which are equally spaced on the logarithmic time axis, and then calculating the strength of the spectral line associated with each respondence time. Our method shares this feature with the collocation method and the multidata method. However, in contrast to these methods, ours does not require matrix inversion and thus avoids mathematical difficulties associated with such an inversion (such as, for example, occasionally generating troublesome negative respondence times). We calculate the intensity (i.e. the strength) of the kth spectral line corresponding to the kth respondence time τ_k, from all source data lying within a fixed time interval (window 1) around τ_k (Fig. 1). The contributions to the strength of this line arising

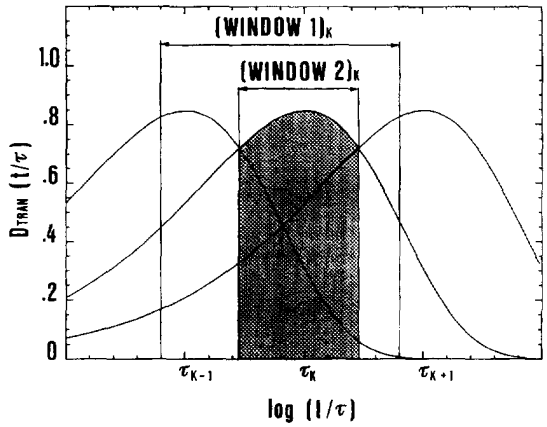

Fig. 2. Definition of window 2 (the modeling window).

from the presence of neighboring spectral lines is taken into account by making appropriate assumptions concerning the spread of the neighboring lines which will make non-negligible contributions (window 2) (Fig. 2). The spectrum is calculated by proceeding from the low end towards the high end of the response, again making appropriate assumptions. Finally, the crude distribution of spectral lines obtained in the first pass is improved by iteration.

As mentioned previously, we shall demonstrate our method for the case of the shear relaxation modulus. The method can be easily adapted to dealing with the tensile relaxation modulus or the tensile creep compliance or, for that matter, with any other response to the imposition of a strain or a stress as a step function of time (Tschoegl, 1989, Chapter 11).

THE ALGORITHM

The theory of linear viscoelastic behavior describes the shear relaxation modulus by the relation

$$G(t) = \{G_e\} + (G_g - \{G_e\}) \int_0^\infty h(\tau) \exp - t/\tau \, \mathrm{d} \ln \tau, \tag{1}$$

where $h(\tau)$ is the (normalized) continuous relaxation spectrum and G_g and G_e are the instantaneous and the equilibrium modulus, respectively. The braces signify that $\{G_e\} = G_e$ when the modulus describes an arrheodictic material, and that $\{G_e\} = 0$ when the material is rheodictic. (The term rheodictic refers to a material showing steady-state flow.) Dividing by $G_g - \{G_e\}$ yields

$$g(t) = \{g_e\} + \int_0^\infty h(\tau) \exp - t/\tau \, \mathrm{d} \ln \tau, \tag{2}$$

where $g(t)$ and g_e are the normalized relaxation modulus and equilibrium modulus, respectively.

The source data are assumed to be available as a set of M discrete data points

$$G_j \in \{t_j, G(t_j); \quad j = 1, 2, \ldots, M\}. \tag{3}$$

Each of these data points can be normalized by the difference between the largest G_1, and the smallest point G_M, to yield the set

$$g_j \in \{t_j, g(t_j);\quad j = 1, 2, \ldots, M\}. \tag{4}$$

Now, the modulus can be expressed alternatively by a discrete set of (normalized) spectral lines h_i. In terms of these we have

$$G(t) = \{G_e\} + (G_g - \{G_e\}) \sum_{i=1}^{i=n} h_i \exp - t/\tau_i \tag{5}$$

or, in normalized form,

$$g(t) = \{g_e\} + \sum_{i=1}^{i=n} h_i \exp - t/\tau_i. \tag{6}$$

We intend to determine, from the set of source data $\{g_j; j = 1, 2, 3, \ldots, M\}$, a set of spectral lines $\{h_i; i = 1, 2, 3, \ldots, n\}$ which will faithfully reproduce the modulus $G(t)$. In proceeding to explain how this is done, we initially use the continuous representation (2), instead of its discrete equivalent (6), because this simplifies the presentation.

We begin by splitting the integral in eqn (2) to obtain

$$g(t) = \{g_e\} + \int_0^{\tau_a} h(\tau) \exp - t/\tau \, \mathrm{d} \ln \tau + \int_{\tau_a}^{\tau_k^-} h(t) \exp - t/\tau \, \mathrm{d} \ln \tau + h(\tau_k) \exp - t/\tau_k + \int_{\tau_k^+}^{\infty} h(\tau) \exp - t/\tau \, \mathrm{d} \ln \tau. \tag{7}$$

Let the kernel in the integrals in eqn (7) be represented by the function $K(t) = \exp - t/\tau$. Figure 1 shows a plot of $K_k = \exp - t/\tau_k$ as a function of $\ln t/\tau_k$. The broken line represents the tangent to $K_k(t)$ at $\ln t/\tau_k = 0$. From the behavior of the kernel we can draw two immediate conclusions. First,

$$K_k(100\tau_k) = 3.72 \times 10^{-44} \simeq 0. \tag{8}$$

Second, the logarithmic time interval $-0.6 < t/\tau_k < 0.4$ defines the region over which $K_k(t)$ shows its largest time dependence. We call this interval window 1. The interval from which data points will be drawn from the set of source data to calculate the kth spectrum line depends on the number of lines per logarithmic decade of time. We call this interval window 2. Figure 2 shows $D_{\mathrm{TRAN}}(t) = K'(t)$, the derivative of $K(t)$, as a function of $\ln t/\tau_k$ for $\tau = \tau_{k-1}$, τ_k and τ_{k+1}. The intersections of the central derivative with its neighbors to the left and to the right, designated by t_l and t_u (for *lower* and *upper*) are given by

$$t_l = \frac{\tau_k \tau_{k-1}}{\tau_k - \tau_{k-1}} \ln \frac{\tau_k}{\tau_{k-1}} \tag{9}$$

and

$$t_u = \frac{\tau_{k+1} \tau_k}{\tau_{k+1} - \tau_k} \ln \frac{\tau_{k+1}}{\tau_k}. \tag{10}$$

If P is the number of spectral lines per decade of $\log t$, then we have $\log \tau_{k+1} - \log \tau_k = 1/P$ and, therefore,

$$t_l = \frac{2.303}{P(10^{1/P} - 1)} \tau_k \tag{11}$$

and

$$t_u = \frac{2.303 \times 10^{1/P}}{P(10^{1/P}-1)} \tau_k. \tag{12}$$

Therefore, the spread of window 2 is given by $[t_l, t_u]$. The width of the window decreases as the number of spectral lines increases. Accordingly,

$$\lim_{P \to \infty} \text{window } 2 = 0 \tag{13}$$

marks the transition from the discrete to the continuous form of the representation of $G(t)$.

The third conclusion we can draw from Fig. 1 states that window 2 must not be larger than window 1. Outside of window 1, the kth spectral line cannot handle data points because its contribution on the right is virtually zero, and on the left it approaches a constant value. On the other hand, we must have at least one discrete data point lying within window 2. This realization allows us to determine the optimum number of spectrum lines per logarithmic decade to be chosen. This number must be such that the width of window 2 approaches (but does not exceed) the width of window 1. The number can be found by solving the transcendental equations (11) and (12). In eqn (11) we let $\log t_l/\tau_k = -0.6$, in eqn (12) we let it be $\log t_u/\tau_k = 0.4$ and solve for the nearest integer P. The smaller of the two solutions gives the desired optimum number of spectral lines per decade, i.e. $P = 2$.

We can now return to eqn (7). Each datum point within window 2 pertaining to the kth spectrum line can be modeled as

$$g_j = \{g_e\} + \int_0^{\tau_a} h(\tau) \exp -t_j/\tau \, \mathrm{d} \ln \tau + \int_{\tau_a}^{\tau_k^-} h(t) \exp -t_j/\tau \, \mathrm{d} \ln \tau + h(\tau_k) \exp -t_j/\tau_k + \int_{\tau_k^-}^{\infty} h(\tau) \exp -t_j/\tau \, \mathrm{d} \ln \tau. \tag{14}$$

By our first conclusion from Fig. 1, if $\tau_a \leqslant t_k/100$, then the first integral in eqn (14) vanishes.

Proceeding now from the continuous to the discrete representation, we write

$$g_j = \{g_M\} + \sum_{i=m}^{i=k-1} h_i \exp -t_j/\tau_i + h_k \exp -t_j/\tau_k + \sum_{i=k+1}^{i=n} h_i \exp -t_j/\tau_i + \Delta_j. \tag{15}$$

In the equation above, m is the discrete counterpart of τ_a and is given by $m = k-2n-1$. The term Δ_j has been added to take into account the absolute error introduced by switching from the continuous to the discrete representation. Using the abbreviation

$$\mathscr{Z}(t_j) = \{g_M\} + \sum_{i=m}^{i=k-1} h_i \exp -t_j/\tau_i + h_k \exp -t_j/\tau_k + \sum_{i=k+1}^{i=n} h_i \exp -t_j/\tau_i, \tag{16}$$

where $\mathscr{Z}(t_j)$ denotes the theoretical (error free) value of the normalized experimental datum point g_j, the term Δ_j can be expressed as

$$\Delta_j = g_j - \mathscr{Z}(t_j). \tag{17}$$

To avoid the instability problems caused by the large difference in magnitude of modulus on both sides of window 2 we introduce the relative error of approximation [for details see Emri and Tschoegl (1994)]

$$\delta_j = \frac{\Delta_j}{\mathscr{Z}(t_j)} = \frac{g_j - \mathscr{Z}(t_j)}{\mathscr{Z}(t_j)}. \tag{18}$$

The sum Q_k of the squares of δ_j within window 2 is

$$Q_k = \sum_{j=s_{k,l}}^{j=s_{k,u}} \delta_j^2 \tag{19}$$

where $s_{k,l}$ and $s_{k,u}$ are the first and the last discrete points in window 2 belonging to the kth spectrum line. Minimizing the error according to

$$\frac{\partial Q_k}{\partial h_k} = 0, \tag{20}$$

where h_k is the kth spectrum line, leads to the expression from which the strength of the kth spectral line is to be obtained,

$$\sum_{j=s_{k,l}}^{j=s_{k,u}} \frac{g_j - \mathscr{Z}(t_j)}{[\mathscr{Z}(t_j)]^3} g_j \exp - t_j/\tau_k = 0. \tag{21}$$

Using the abbreviation

$$\mathscr{I}(t_j) = \{g_M\} + \sum_{i=m}^{i=k-1} h_j \exp - t_j/\tau_i + \sum_{i=k+1}^{i=n} h_i \exp - t_j/\tau_i, \tag{22}$$

and eqn (16) in addition, we obtain the equation

$$\sum_{j=s_{k,l}}^{j=s_{k,u}} \frac{g_j - [\mathscr{I}(t_j) + h_k \exp - t_j/\tau_k]}{[\mathscr{I}(t_j) + h_k \exp - t_j/\tau_k]^3} g_j \exp - t_j/\tau_k \equiv 0. \tag{23}$$

This equation must be satisfied to minimize the sum of squares of the relative quadratic errors Q_k in the kth window. It must be solved numerically by iteration for it cannot be made explicit for h_k as is possible when minimizing the absolute error (Emri and Tschoegl, 1993a,b; Tschoegl and Emri, 1992). We therefore now recast (23) in a form in which it becomes suitable for recursion. We let

$$h_k^{(i+1)} = \frac{\mathscr{A}[h_k^{(i)}]}{\mathscr{B}[h_k^{(i)}]} \tag{24}$$

where $h_k^{(i)}$ is the value of h_k obtained in the ith iteration,

$$\mathscr{A}[h_k^{(i)}] = \sum_{j=s_{k,l}}^{j=s_{k,u}} \frac{g_j - \mathscr{I}(t_j)}{[\mathscr{I}(t_j) + h_k^{(i)} \exp - t_j/\tau_k]^3} g_j \exp - t_j/\tau_k \tag{25}$$

and

$$\mathscr{B}[h_k^{(i)}] = \sum_{j=s_{k,l}}^{j=s_{k,u}} \frac{[\exp - t_j/\tau_k]^2}{[\mathscr{I}(t_j) + h_k^{(i)} \exp - t_j/\tau_k]^3} g_j. \tag{26}$$

The starting set of spectrum lines for the iteration is $\{h_k^{(1)} = h^{(1)}(\tau_k); k = 1,2,\ldots,n\}$. This starting set is obtained in a first sweep through the data using the method detailed in the

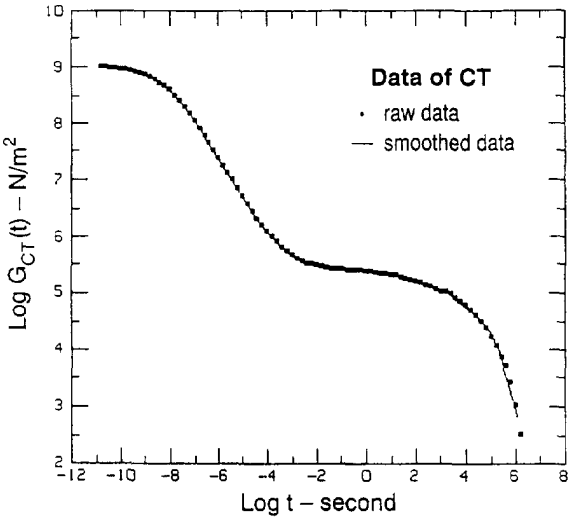

Fig. 3. Relaxation modulus log $G_{CT}(t)$ as function of log t.

paper (Emri and Tschoegl, 1993a,b). For subsequent sweeps we then use the method just described. The iteration is broken off when an appropriately chosen limit of the absolute difference between the new and the preceding square relative error Q_k has been reached.

RESULTS

We demonstrate the power of the algorithm by obtaining the distribution of spectral lines from the experimental data obtained by Catsiff and Tobolsky (1955) (CT data). The data has been first converted as described in the Introduction. In this form they are tabulated in Tschoegl (1989, p. 40) and are presented in Fig. 3. The solid line represents a spline function (de Boer, 1978) through the data. Figure 4 shows the relaxation spectrum $H_{CT}(\tau)$ calculated from these data, using the presented method.

The reconstruction of the shear relaxation modulus $G(t)$ from the calculated spectrum $H_{CT}(\tau)$, using the relation (5) is compared with the spline function through the original

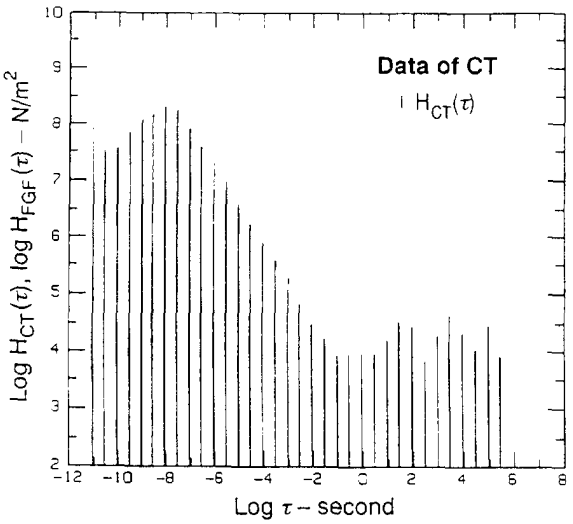

Fig. 4. Relaxation spectrum log $H_{CT}(\tau)$ as function of log τ.

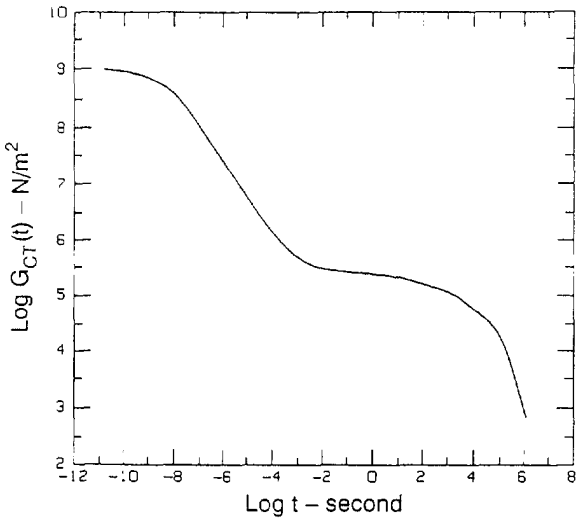

Fig. 5. Reconstruction of log $G_{CT}(t)$ from $H_{CT}(\tau)$, compared with the spline function through the experimental data, as functions of log t.

experimental data in Fig. 5. Both curves can not be distinguished within the resolving power of the plot.

Knowing the spectrum $H(\tau)$ in addition to the viscoelastic constants one can generate from it the response to any desired type of excitation. In order to demonstrate this we first calculate $G'_{CT}(\omega)$ and $G''_{CT}(\omega)$ from $H_{CT}(\tau)$ using the relations (Tschoegl, 1989, Chapter 6, Section 3)

$$G'_{CT}(\omega) = \sum_{i=1}^{i=N} H_{CT}(\tau_i) \frac{\omega^2 \tau_i^2}{1+\omega^2 \tau_i^2} \tag{27}$$

and

$$G''_{CT}(\omega) = \sum_{i=1}^{i=N} H_{CT}(\tau_i) \frac{\omega \tau_i}{1+\omega^2 \tau_i^2}. \tag{28}$$

$G'_{CT}(\omega)$ and $G''_{CT}(\omega)$ can be than interconverted to storage compliance $J'_{CT}(\omega)$ and loss compliance $J''_{CT}(\omega)$, using the relations (Tschoegl, 1989, p. 329)

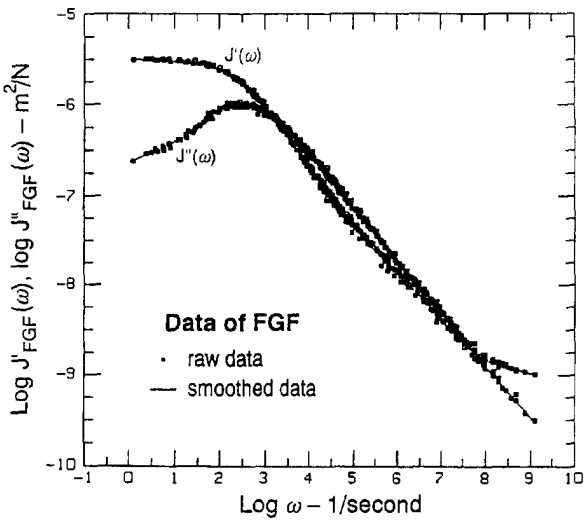

Fig. 6. Storage compliance log $J'_{FGF}(\omega)$ and loss compliance log $J''_{FGF}(\omega)$, as functions of log ω.

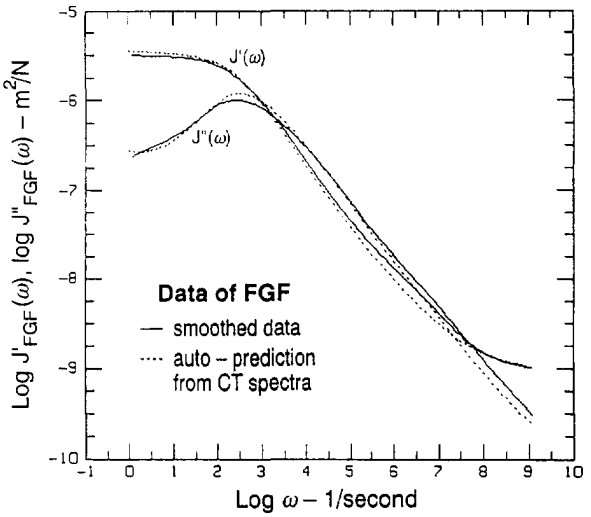

Fig. 7. Smoothed $J'_{FGF}(\omega)$ and $J''_{FGF}(\omega)$ data compared with $J'_{CT}(\omega)$ and $J''_{CT}(\omega)$ derived from $H_{CT}(\tau)$.

$$J'(\omega) = \frac{G'(\omega)}{[G'(\omega)]^2 + [G''(\omega)]^2} \tag{29}$$

and

$$J''(\omega) = \frac{G''(\omega)}{[G'(\omega)]^2 + [G''(\omega)]^2}. \tag{30}$$

$J'_{CT}(\omega)$ and $J''_{CT}(\omega)$ are compared with the experimental data obtained by Fitzgerald *et al.* (1953) (FGF data). The comparison is presented in Fig. 7. $J'_{CT}(\omega)$ and $J''_{CT}(\omega)$, represented as broken lines, are compared with the spline functions through the experimental data $J'_{FGF}(\omega)$ and $J''_{FGF}(\omega)$, shown as solid lines. The original FGF data are shown in Fig. 6. The agreement between the prediction and the spline function through the experimental data is excellent.

CONCLUSION

In this paper we have presented the algorithm for evaluation of relaxation line spectra from experimental data. The algorithm can be easily modified for the assessment of retardation spectra. The algorithm essentially utilizes the fact that the kernel functions resemble step functions. Slightly different codes are used for each kernel function, as presented elsewhere (Emri and Tschoegl, 1993a,b).

We feel that we have demonstrated that the proposed algorithm is indeed capable of generating the underlying line spectra from the experimental data without producing negative lines that are physically unacceptable.

Acknowledgements—The authors gratefully acknowledge support of this work by the Slovene Ministry of Science under Grant P2-1131-782, and partial support by the California Institute of Technology.

REFERENCES

Baumgaertel, M. and Winter, H. H. (1989). *Rheol. Acta* **28,** 510–520.
Catsiff, E. and Tobolsky, A. V. (1955). *Colloid Sci.* **10,** 375–392.
Cost, T. L. and Becker, E. B. (1970). *Int. J. Numer. Meth. Engng* **2,** 207–212.
de Boer, C. (1978). *A Practical Guide to Splines.* Springer-Verlag, NY.
Elster, C. and Honercamp, J. (1991). *Macromolecules* **24,** 310–314.
Elster, C. and Honercamp, J. (1992). *J. Rheol.* **36,** 911–927.
Emri, I. and Tschoegl, N. W. (1993a). *Rheol. Acta* **32,** 311–321.
Emri, I. and Tschoegl, N. W. (1993b). *Rheol. Acta.* **32,** 322–327.

Emri, I. and Tschoegl, N. W. (1994). *Rheol. Acta.* **33,** 60–70.
Emri, I. and Tschoegl, N. W. (1995). In preparation.
Ferry, J. D. (1980). *Viscoelastic Properties of Polymeric Materials.* Wiley, NY.
Fitzgerald, R. E., Grandine, L. D., Jr and Ferry, J. D. (1953). *J. Appl. Phys.* **24,** 650–655.
Honercamp, J. (1989). *Rheol. Acta* **28,** 363–371.
Honercamp, J. and Weese, J. (1989). *Macromolecules* **22,** 4372–4377.
Janzen, J. and Scanlan, J. (1992). Submitted to *Rheol. Acta.*
Kamath, V. M. and Mackley, M. R. (1989). *J. Non-Newt. Fluid Mech.* **32,** 1199–1204.
Laun, H. M. (1986). *J. Rheol.* **30,** 459–467.
Orbey, N. and Dealy, J. M. (1991). *J. Rheol* **35,** 1035–1049.
Schapery, R. A. (1962). *Proc. 4th U.S. National Congress Appl. Mech.* **2,** 1075–1081.
Tobolsky, A. V. and Murakami, K. (1959). *J. Polymer Sci.* **40,** 443–452.
Tschoegl, N. W. (1989). *The Theory of Linear Viscoelastic Behavior.* Springer-Verlag, NY.
Tschoegl, N. W. and Emri, I. (1992). *Int. J. Polym. Mater.* **18,** 117–127.